NANO LETTERS

pubs.acs.org/NanoLett Letter

Interaction Effects and Non-Integer Pseudo-Landau Levels in Engineered Periodically Strained Graphene

Iva Šrut Rakić, Matthew J. Gilbert, Preetha Sarkar, Anuva Aishwarya, Marco Polini, Vidya Madhavan,* and Nadya Mason*

Cite This: *Nano Lett.* 2025, 25, 41−47 Read Online

ACCESS | Metrics & More | Article Recommendations | Supporting Information

ABSTRACT: Strain superlattices (SL) in 2D materials like graphene provide an ideal test bed for generating flat bands and exploring the effects of strong correlations. Here we report STM/STS measurements on an engineered SL generated by placing graphene on a periodic array of silica nanospheres. A pseudomagnetic field as high as 55 T is observed along with the formation of pseudo-Landau levels (pLLs), not only at the expected integer values but also at fractional values. In regions where the Fermi energy intersects the zeroth pLL, we observe that this pLL splits. Using tight binding calculations, we show that our system supports formation of quasi-flat bands. We are also able to simulate the strain induced pLL splitting and show how on-site interaction may create fractional pLLs. Thus, we have demonstrated a customizable, reproducible, and scalable graphene strain superlattice system that can host a range of different correlation driven states.

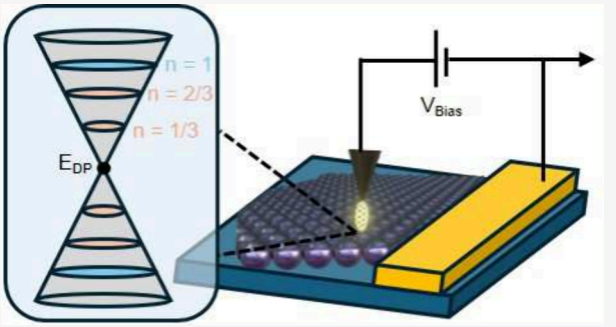

KEYWORDS: *Graphene, Periodic strain, Flat bands, Fractional pseudo-Landau levels, Peak split, Electron−electron interactions*

Strong correlations in two-dimensional electron gases lead to a range of interesting phases such as strange metals,[1] magnetically induced Wigner crystals,[2] fractional quantum Hall (FQH) states[3−5] and unconventional superconductors.[6] Dispersion-less "flat" energy bands are known to enhance correlations,[7−9] due to the reduced kinetic energy of charge carriers. For example, when a strong perpendicular magnetic field is applied to a 2D electron gas, like graphene, a series of quantized density of states called Landau levels are formed.[10,11] The increased Coulomb interactions in these flat energy levels have led to the observation of a fractional quantum Hall effect in low-disordered graphene.[12,13] More recently, unconventional intrinsic superconductivity was observed in magic angle twisted bilayer graphene due to enhanced correlation effects from the superlattice potential.[6,14] However, engineering flat bands using 2D moiré superlattices has limitations in terms of material choice, precise control of the twist angle, and the inability to induce "ideal" flat bands.[15] This calls for more robust techniques for realizing flat bands in 2D materials.

Mechanical strain can also generate flat bands in graphene.[16−18] Nonuniform strain in naturally formed graphene nanobubbles has been shown to give rise to pseudo magnetic fields (PMFs) in excess of 300 T, and corresponding integer pseudo-Landau levels (pLL).[19] Imposing a periodic strain of specific trigonal geometry on graphene can induce a C_{2Z} symmetry breaking leading to gap opening, quasi-flat band formation with strong correlations, and rich edge-state physics.[15,16,20,21] Strained graphene should also be able to host FQH phases or even superconductivity if Coulomb interactions are introduced.[22] Although pLLs were observed at both integer and fractional values in strongly strained graphene CVD grown on copper substrates,[23] the strain was released and PMF effects were significantly diminished upon transfer onto insulating silica substrates, making this strain technique incompatible with standard CMOS device fabrication. The exact role of Coulomb interactions in generating the fractional energy levels was also not well understood due to complications posed by conducting substrates.

To incorporate the effects of strain globally in graphene devices, it is important to generate periodic strain "superlattice" potentials. Buckled graphene superlattices have been observed to naturally form on substrates such as $NbSe_2$ due to thermal cycling.[24] Such periodically buckled graphene has been shown to host nearly flat bands and signatures of correlated states. Furthermore, these strained systems also show valley polarization i.e. opposite signs of PMF in the K and K' valleys, necessary for valleytronics.[25,26] Graphene strain superlattices

Received: July 23, 2024
Revised: November 21, 2024
Accepted: December 10, 2024
Published: December 16, 2024

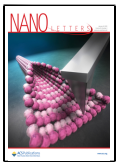

https://doi.org/10.1021/acs.nanolett.4c03542
Nano Lett. 2025, 25, 41−47

made by thermal cycling, however, are not scalable, and difficult to reproduce. They are also predominantly made on a metallic substrate which hinders their use as a potential platform to study strong correlation effects in topological bands.[15]

This calls for more controlled approaches to engineering periodic strain in graphene on a dielectric substrate. One possibility is to place graphene on nanopatterned substrates.[27−30] Patterned substrates can induce periodic electrostatic potentials in graphene, resulting in emergence of multiple Dirac cones, fractal mini-gaps of the Hofstadter spectrum, and even flattening of the Dirac cone.[27,28] They may also act as a source of 3D deformation and generate a strain superlattice, with a tunable strain depending on their size.[31] Transport studies on monolayer graphene layered on quasi-periodic, hexagonal arrays of silica nanospheres have demonstrated the formation of a strain superlattice.[29,31] However, to fully comprehend the effects of local variations of strain, and hence PMF, on the electronic properties, nanoscale studies are needed.

In this work, we report low temperature scanning tunneling microscopy (STM) and spectroscopy (STS) studies of graphene stacked on an array of 20 nm SiO_2 nanospheres (NSs) (Figure 1(a)). STS measurements show the formation of strain-induced pLLs and a spatially varying PMF profile with values as large as 55 T on top of the nanospheres. In regions where the Fermi energy moves across the zeroth pLL peak, the peak splits, resulting in a low-energy gap. The width of this gap

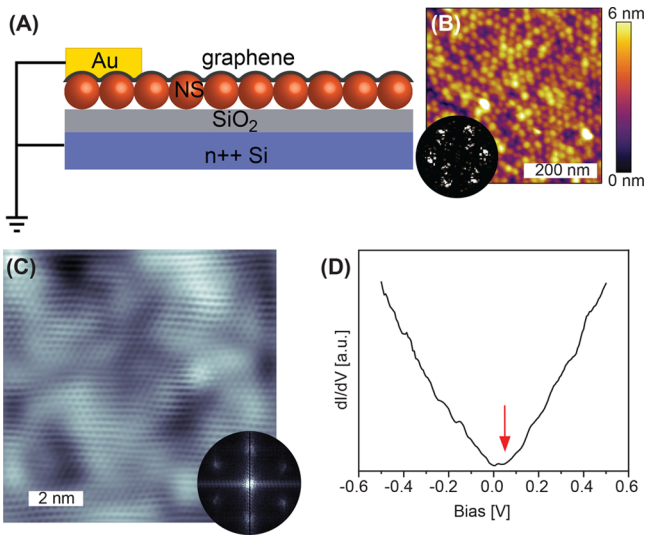

Figure 1. Graphene-covered NSs system: (a) A schematic representation of the sample geometry and sample setup for the STM and STS measurements at 4.5 K. (b) AFM topography of the sample taken prior to insertion in a UHV chamber. Inset shows a Fourier transform of this AFM image after masking the NSs and applying a Gaussian filter to smooth the mask. The visible periodicity corresponds to a real space superlattice of 21.6 nm. (c) An atomically resolved STM topography of the flat graphene on SiO_2, with a Fourier transform of the image shown in inset confirming the hexagonal structure. As previously reported, such areas exhibit low level corrugation in STM, which is not purely topographical but also partially attributed to charge puddles.[33] (d) STS point spectrum of graphene on flat SiO_2. Red arrow indicates the position of the Dirac point, while the gap-like feature at Fermi level corresponds to phonon-mediated inelastic tunneling.[33]

varies with the spatial variation of the PMF. Although this effect has been theoretically predicted by earlier studies[24] it was never experimentally observed. Finally, we also observe the emergence of pLLs at fractional values. Our theoretical calculations elucidate the role of the Coulomb onsite and next-nearest neighbor interactions in the formation of fractional pLLs. Understanding the effect of electron−electron interactions on generating fractional pLLs had been missing in previous studies. More broadly, our experimental data and numerical calculations are consistent with significant flattening of the electronic bands over the entire k space. Thus, we are able to demonstrate a reproducible, scalable strain superlattice in graphene where periodic variations of PMF drive band flattening, increasing Coulomb interactions and thus leading to signatures of strongly correlated phases like fractional pseudo-Landau levels. Unlike previous graphene strain superlattices, which were generated as a byproduct of growth procedures, the strain superlattices in our graphene systems have been designed and engineered using custom substrates, and thus have been reproducible and tunable. The conducting nature of the substrates in previous studies meant that the tunneling and transport response of the strained graphene layer merged with that of the substrate, and there was no scope for gate-induced carrier density tunability - a basic requirement for CMOS device technology. The insulating silica substrates in this study meet this criterion for CMOS compatibility, and transport signatures of strain superlattices have been successfully observed in these systems.[29]

SiO_2 NSs deposited on Si wafer have an average 20 nm diameter and form a quasi-periodic hexagonal close-packed pattern[30] as seen from large scale atomic force microscopy (AFM) image (Figure 1(b)). The average graphene corrugation, i.e. draping between two NSs, measured with AFM is 4.47 ± 0.05 nm. While graphene does not perfectly follow the NS shape, by using 20 nm NSs we ensured to minimize appearance of folds while maximizing strain.[30] NSs tend to cluster in close-packed areas containing hundreds of NSs separated by bare substrate. Since graphene covers both those regions this allows us the choice to position the STM tip on either corrugated or flat graphene (cf. Supplementary Figure 1). Atomically resolved images of flat regions reveal the honeycomb pattern characteristic of graphene (Figure 1(c)). We attribute these regions to areas without NSs such that graphene covers a flat SiO_2 substrate. These regions also exhibit a standard noninteracting density of states (DOS) that is visible in STS with a dip at 40 meV (Figure 1(d) red arrow) corresponding to the charge neutrality point (CNP) i.e. Dirac point position[32,33] indicating an electron doped graphene.

We now focus our attention on the graphene-covered close-packed NS regions(Supplementary Figure 1) and their local density of states (LDOS) (Figure 2). The high-resolution STM image of graphene-covered NS in Figure 2(a) shows that graphene forms complex bubble and fold-like shapes as it bends over the NS with evident deformations in the graphene unit cell (cf. Supplementary Figure 2). Atomic resolution images reveal a local transition from a honeycomb to a triangular pattern (cf. Supplementary Figure 2(b)). This sublattice polarization of the electronic wave function has been previously shown to be a hallmark of PMFs[24,25,34−36] and indicates PMF sign switching along with a zero crossing.

Examining the LDOS of the graphene-covered NS shown in Figure 2(a) we find that the spectra in this region are highly location dependent. We first focus on the two extremes, the

https://doi.org/10.1021/acs.nanolett.4c03542
Nano Lett. 2025, 25, 41−47

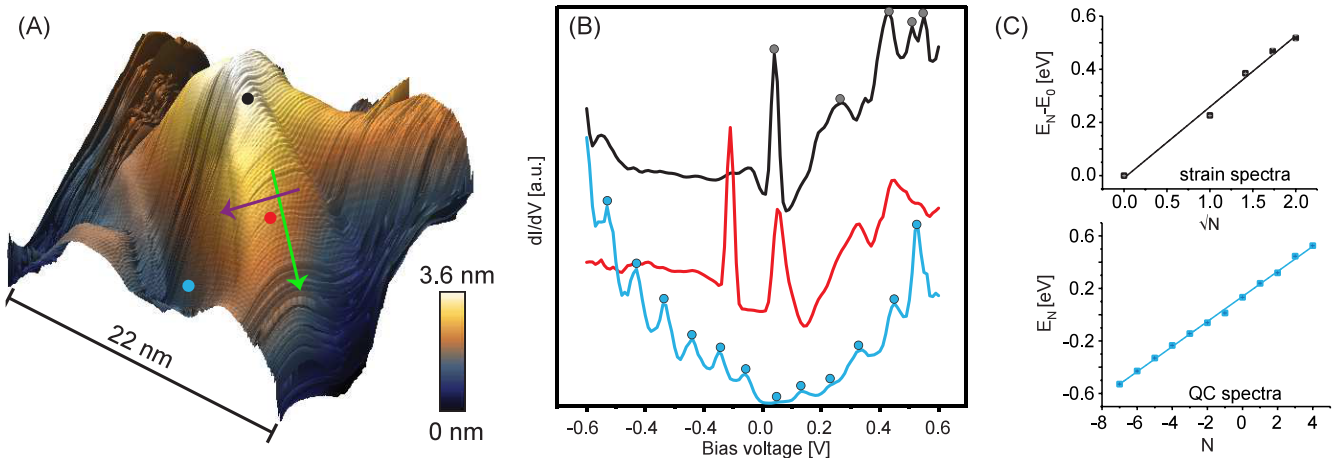

Figure 2. STM/STS of graphene-covered NS: (a) 3D STM topography of graphene-covered NS. Green and purple arrows mark directions along and transverse to the ridge. (b) STS point spectra taken at color-coded positions marked on (a) reveal three distinct LDOS peak behaviors: single pronounced $N = 0$ peak (black), $N = 0$ peak split in two (red) and a sequence of equidistant peaks (blue). Dots mark the position of peaks used to fit data in (c). To fit the actual peak positions we used negative of second derivative of this data (cf. Supplementary Figure 2). The sequence of pLLs on the side of the NS (red) corresponds to a PMF of 29 ± 1 T. (c) Upper panel: Plot of peak energy position versus square root of index number N and linear fit for the black spectrum in (b). Linear fit yields a local PMF of 54 ± 1 T, a value significantly larger than the PMF obtained from magneto-transport measurements on samples with the same geometry, which represent a macroscopically averaged value.[29] Lower panel: Plot of peak energy position versus peak index N and linear fit for the blue spectrum in (b). The electrons in this region are trapped in a PMF-induced potential well due to the significant spatial gradient of the PMF. Strain-induced quantum confinement (QC) has been previously observed in buckled graphene on $NbSe_2$[24] and in graphene ripples on Cu foil.[37]

apex of the NS and the valley between NSs, indicated by the black and blue dots as shown in Figure 2(b). Spectrum taken at the apex of the NS (black) show a prominent peak at 41 meV and a sequence of weaker peaks. The energy E_N of the N-th pLL is given by the relation $E_N = E_D + \mathrm{sgn}(N)v_F\sqrt{2e\hbar|N|B_{\mathrm{PMF}}}$, where E_D is the energy of Dirac point, v_F the Fermi velocity and $\hbar = h/2\pi$.[19] We identify the prominent peak as the $N = 0$ pLL which sits at CNP of the graphene on flat SiO_2 (cf. Figure 1(d)). By plotting E_N–E_0 versus $\sqrt{N}$ and fitting a linear curve (Figure 2(c) upper panel) we get a PMF of 54 ± 1 T. In contrast to the apex, the spectrum taken at the valley between two NSs (blue) is symmetric with an equidistant sequence of peaks spaced approximately by 95 meV. This linear relationship between energy and peak index N, $E_N \sim N$, as shown in the bottom panel of Figure 2(c) is likely due to strain induced confinement.[24] Comparing the equidistant energy levels of $\Delta E = 95\ meV$ to the confinement in quantum dots in 2D semiconductors $\Delta E = \hbar v_F\ \pi\ /W$[24] we estimate approximate quantum dot size of 20 nm which is in accordance with the average distance between two NSs in our system.

While cursory analysis of the peaks and troughs of the NS array yields results consistent with previous work, as we traverse the transition region between the peak and trough of an individual NS, we observe significant deviations. Closer examination of the differential conductance spectrum in Figure 2(b) taken around 5.5 nm from the NS peak (red dot in Figure 2(a)) reveals two prominent peaks at −110 and 57 meV, with an estimated 80 meV gap between them, and seven weaker peaks on either side of energy scale (cf. Supplementary Figure 3). These energetically segregated peaks correspond to the split $N = 0$ peak where the CNP is shifted and lies in between the two peaks at approximately −27 meV (cf. Supplementary Figure 3). To understand the emergence of the split $N = 0$ peak, we plot the spectra along the two directions marked green and purple in Figure 2(a). We focus on the two peaks corresponding to the N = 0 split peak (Figure 3). The distance between peaks (around 0.1 V and −0.1 V) varies with the

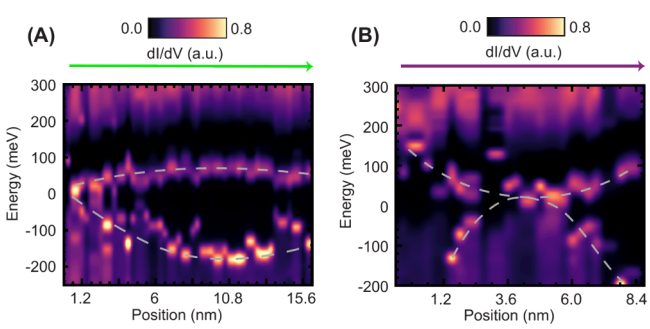

Figure 3. Split $N = 0$ peaks: (a) and (b) Map of STS point spectra taken along the color-coded positions marked with green and purple arrows on Figure 2 (a) respectively. Gray dashed lines are a guide to the eye marking approximate positions of the two peaks we attribute to the $N = 0$ split peak.

STM tip's position on the NS. As the tip scans across the graphene fold in Figure 3(b), the peaks, initially separated by approximately 240 meV, move closer together toward $E = 0$. At the fold's apex, they merge into one peak, but moving the tip away causes them to separate again, increasing the energy gap to around 340 meV. Similar behavior was predicted by theoretical calculations of Mao et al.,[24] which showed that for PMF lower than the critical value, specific for the periodicity of the system, the $N = 0$ peak will split but only for the LDOS of one graphene sublattice. They also calculate that the gap between peaks follows local changes in PMF and is the highest in the regions of lower PMF, in correlation to our data. While their paper does not directly address the origin of the split, we attribute it to a combination of three factors based on their calculations and the work of Milovanović et al.[20] First, progressive band narrowing and flattening occurs with

https://doi.org/10.1021/acs.nanolett.4c03542
Nano Lett. 2025, 25, 41−47

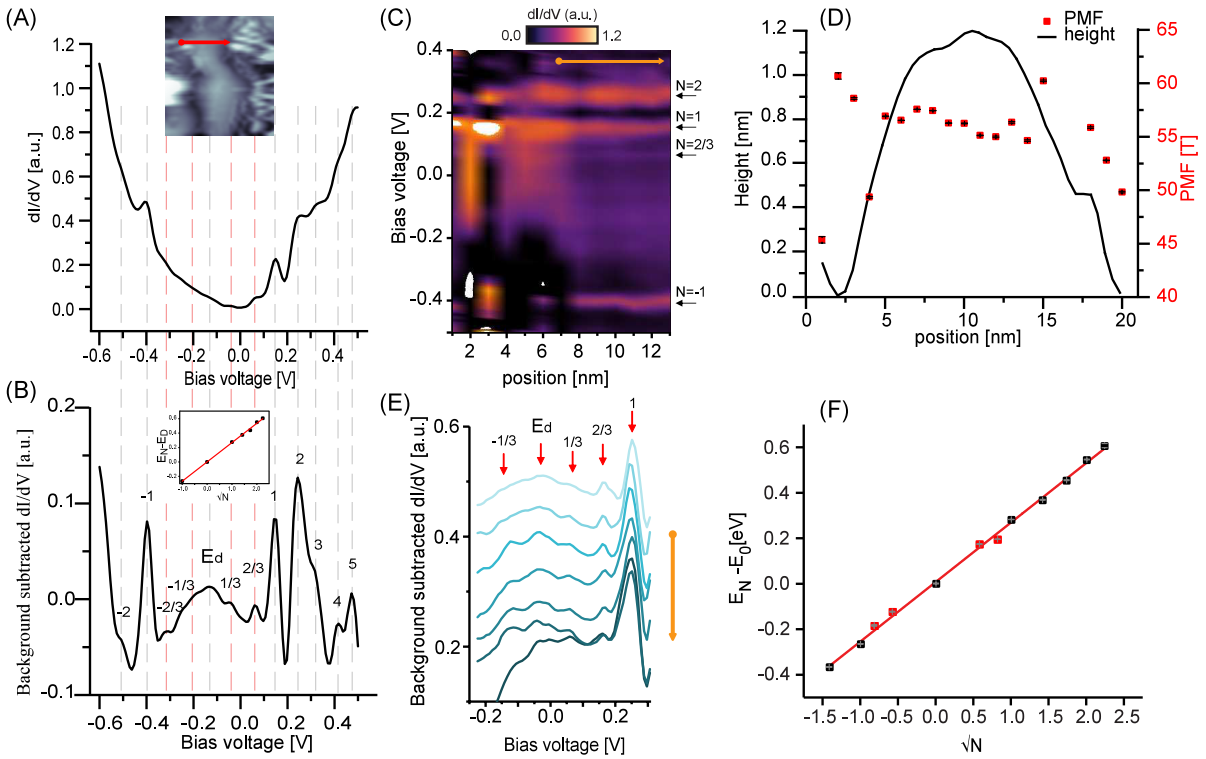

Figure 4. Pseudo Landau levels: (a) A dI/dV point spectrum at 10 nm position from a line scan taken along the marked red arrow in the inset. Inset shows a STM topography of graphene on NS where line scan was taken, representing different sample location than the one in Figure 2. (b) Residual after second polynomial retraction from spectra in (a). Inset shows the energy, $E_N - E_D$, versus $\sqrt{N}$ of integer pLLs marked in (b). Dirac point was determined as a halfway point between $N = 1$ and $N = -1$. Fitting a linear fit we get a local PMF of 52 ± 3 T. (c) A full map of dI/dV spectra taken along the red arrow in (a) with second polynomial retraction applied. Black arrows mark the $N = -1$, 2/3, 1, and 2 pLLs. (d) A height profile of the crest region from inset in (a) versus calculated PMF at that position. Two STS point missing at 16 and 17 nm could not be processed in this manner as their shape deviates from parabolic. The PMF diminishes on the sides of the graphene-covered NS structure indicating the onset of a region characterized by highest strain gradient. (e) Residual after second polynomial retraction presented in 4(c) shown in a narrower bias range, for a point spectra marked by an orange arrow in 4c. The fractional peaks appear in a region with a constant PMF (cf. Figure 4(d)), in addition to being clearly segregated from the valley between two NSs, where quantum confined states typically appear (cf. Figure 2(b)). (f) E_N versus $\sqrt{N}$ fit for all detected peaks including fractional pLLs which are marked in red.

increased strain. Second, higher $N > 0$ bands reach "flatness" at lower PMFs compared to $N = 0$[20] and therefore show no splitting even when the $N = 0$ level does. Third, the PMF breaks the sublattice symmetry localizing the $N = 0$ electronic wave function on a single sublattice for a particular PMF sign (cf. Figure 1c in Milovanović et al.[20] and Suppl. Figure 2b). We hypothesize that as we move from the side of the sphere to its crest, transitioning from a region of lower to higher PMF, we observe the continuous narrowing of the split $N = 0$ band as we move to a region of higher PMF, ultimately resulting in a single peak. We note that while our system deviates from the perfect superlattice used in their calculations, Mao et al. showed that flat bands are stable even when they introduce high levels of disorder.[24]

Beyond the splitting of the $N = 0$ peak, we observe the existence of pLLs at noninteger values. Figure 4(a) shows a representative dI/dV spectrum obtained along the line marked by a red arrow corresponding to the point of maximal strain within the local coordinates of the array addressed by the tip. The spectrum has a parabolic shape with several noticeable peaks. To better visualize the peaks we subtract a parabolic background from the spectrum[19,23] and plot resulting data in Figure 4(b) (cf. Supplementary Figure 4 for more detail). Peaks at energies proportional to $\sqrt{N}$ with $N = 0, \pm1, \pm2, 3, 4,$ and 5 are clearly visible. The $N = 0$ peak corresponding to Dirac point now sits around −130 meV, constituting an approximate 170 meV shift in position compared to flat unstrained graphene on an SiO_2 substrate. The shift in the energetic position of the $N = 0$ peak is due to a difference in local doping brought about by trapped charge in SiO_2 (cf. Supplementary Figure 5).[32,38] These integer pLLs are visible across the entire scan of the graphene-covered NS, as is visible from an intensity plot of the STS line scan shown in Figure 4(c). The variation in the calculated PMF across the presented line scan, shown in Figure 4(d), is homogeneous near the crest region. This homogeneity of PMF over length scales several times larger than the magnetic length is extremely important as it can affect the occurrence of pLLs vs effects of quantum confinement.[24,26,34,35]

We find additional peaks at energies proportional to square root of fractional numbers ±1/3 and ±2/3, as shown in Figure 4(b). By fitting the fractional pLLs to an E_N versus $\sqrt{N}$ together with the integer pLLs we show that they follow the same linear trajectory (Figure 4(f) red points). The resultant linear trajectory is crucial as this is a clear indication that the peaks cannot be interpreted as states resulting either from quantum confinement[24] or from interference of opposite propagating Hall states.[37]

If the noninteracting relation between filling factor and LL index $\nu = 4(N + 1/2)$ holds when the interaction is included,

https://doi.org/10.1021/acs.nanolett.4c03542
Nano Lett. 2025, 25, 41−47

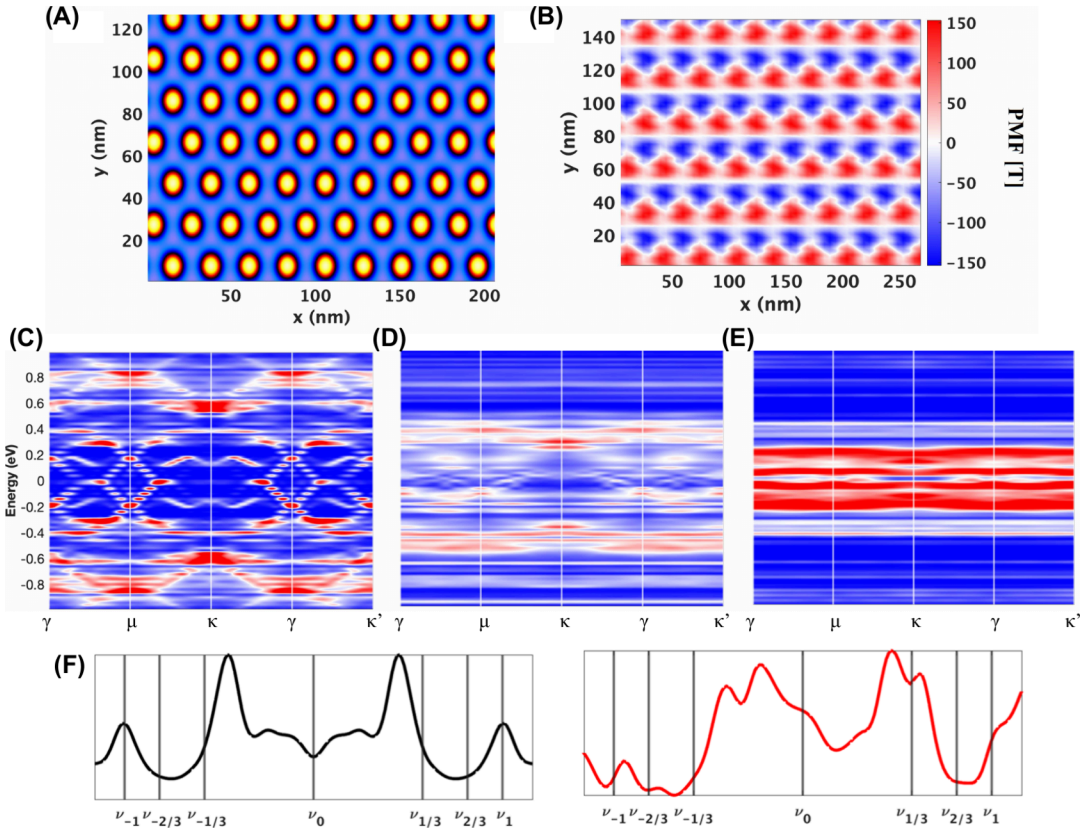

Figure 5. Tight-Binding Calculations of Graphene Strain Superlattice: (a) Depiction of the distribution of 20 nm Gaussian shaped nanospheres implemented in the calculation visualized in continuous configuration prior to discretization. We observe a clear hexagonal close packed configuration with 20 nm of center to center separation. Gaussian peak height can be varied to simulate different strains and is specified for each panel (b) The calculated pseudomagnetic field distribution arising from the strain modified bond lengths in the graphene corresponding to a Gaussian peak of 4 nm. The PMF in the system is significant in magnitude, in the order of ±130 T at peak value that occurs when the gradient of the strain tensor is maximum, and reaches zero magnitude directly on top of the individual NSs. Plot of the calculated band structure in high symmetry directions for the (c) unstrained 20 nm superlattice with (d) 4 nm peak height nanospheres and (e) 5 nm peak height nanospheres where colors denote high (red) and low (blue) intensity values. As the nanosphere height is increased, we observe a gradual flattening of the bands in addition to gaps opening between different groupings of bands. Naturally, as the bands become flatter, one expects to find stronger many-body interactions. (f) Plot of the local density of states (LDOS) of strained graphene covering a NS in the nanosphere lattice at the peak position of the pseudomagnetic field or, x_0 = 75 nm and y_0 = 63 nm. We show comparison between the weakly interacting case, U_{OS} = 0 eV (black), and the strongly interacting case, U_{OS} = 9.3 eV (red).

then our measured pLLs −2/3, −1/3, 1/3, and 2/3 correspond to the filling factors of −2/3, 2/3, 10/3, and 14/3 respectively. In that case the filling factors for both the N = −2/3 and −1/3 pLL would lie within the 0-th pLL, and the N = −1/3 pLL corresponds to a ν = 2/3 that has been theoretically predicted to be a more stable fractional filling factor,[22] though the same picture might not hold when interactions are included.

In order to further elucidate the underlying physics inherent in strained superlattice graphene, we use a tight-binding Hamiltonian of graphene (H_G) and induce strain into the graphene lattice via a deformation field that arises from the presence of Gaussian-shaped insulating NSs, as shown in Figure 5(a).[29,31] We additionally study the behavior of a single Gaussian NS on the properties of the graphene sheet (cf. Supplementary Figure 6) to distinguish between strain and superlattice effects. Figure 5(b) shows the calculated pattern of PMF distribution for a NS array with a 4 nm height modulation.

We next show that graphene strained via a nanosphere array exhibits flat bands. In Figure 5(c), we plot the calculated band structure for Gaussian NSs corresponding to the presence of a superlattice of an extended period but with no modification to the bond lengths of graphene (i.e., no strain) which shows the expected cloning of the graphene Dirac points. In Figure 5(d), we repeat the calculation for a strained system, using an undulation height of 4 nm corresponding to the experimental system.

The increase in the bond length corresponding to the undulation of the graphene on top of the NSs causes the band structure to retain the superlattice Dirac points, however, the bands clearly have significantly less gradient in the energy bands throughout the Brillouin zone when compared to the unstrained superlattice case in Figure 5(c). Under these conditions, the low energy band flatness implies a quenched dispersion relation and the associated potential to find enhanced Coulomb interactions associated with the appearance of fractional phases.[16−18,39] In Figure 5(e), the height of the nanospheres is increased to 5 nm, the bands structure continues to adiabatically flatten though strained monolayer graphene does not possess the proper terms in the Hamiltonian to be perfectly flat as in the case of twisted bilayer graphene.

https://doi.org/10.1021/acs.nanolett.4c03542
Nano Lett. 2025, 25, 41−47

To include interactions, necessary for the appearance of fractional pLL peaks we follow previous work, where the fractional phase may be represented in a mean-field description.[22,40] We use the interaction Hamiltonian, consisting of the unscreened Coulomb interaction, H_C, an on-site interaction H_{OS} with magnitude U_0, and the next-nearest neighbor (NNN) electron−electron interaction H_{NNN} characterized by the term U_{NNN} (cf. Supplementary). We start by considering only Coulomb interactions for a superlattice of NSs (Supplementary Figure 8). As can be seen in Figure 5(f) our calculations reproduce the splitting in the zeroth LL peak. We note that calculations for graphene on a single NS also show clear splitting at positions corresponding to a maximal strain gradient as shown in Supplementary Figure 7.

We next augment the noninteracting graphene Hamiltonian, H_G with the screened, on-site, and next-nearest neighbor Coulomb interactions to determine whether the appearance of fractional levels is plausible given the experimental conditions set forth in this work. First we fix the interaction strength for the NNN interaction to be a fraction of the bare Coulomb interaction or $U_{NNN} = -0.04q^2/4\pi\epsilon a_0$ eV and vary the on-site Coulomb interaction, U_{OS} from $U_{OS} = 0$ eV to the freestanding graphene calculated value of $U_{OS} = 9.3$ eV (Supplementary Figure 9). We now observe additional peaks appearing with the introduction of the interactions to the model (see also Supplementary Figure 8). Although the peak positions do not appear at the expected fillings, our calculations demonstrate how interactions can lead to noninteger peaks in the Landau spectra.

In conclusion, we demonstrated that graphene strained on a quasi-periodic hexagonal array of SiO_2 nanospheres exhibits both integer and noninteger pLLs. Additionally, we show that for certain experimental conditions the $N = 0$ pLL peak splits into two which was theoretically predicted,[24] but not experimentally shown. Tight-binding calculations show that increasing strain adiabatically flattens the low energy electronic bands, which occurs only with the inclusion of nanosphere periodicity. Our simulations indicate that both the splitting and the fractional peaks could arise from interaction effects, though more must be done to understand the nature of the peaks, scaling and possibility to facilitate phenomena such as ferromagnetism, superconductivity or fractional Chern insulators.[15,17,22] We believe that our engineered and device fabrication compatible approach of periodic straining is not only a good platform for investigation of interaction related phenomena in graphene, but also presents an ideal means for studying interesting effects of strain in other 2D materials and van der Waals heterostructures.

■ ASSOCIATED CONTENT

Supporting Information

The Supporting Information is available free of charge at https://pubs.acs.org/doi/10.1021/acs.nanolett.4c03542.

Methods, additional experimental data and processing information, details of theoretical calculations, and additional theoretical calculations (PDF)

■ AUTHOR INFORMATION

Corresponding Authors

Vidya Madhavan − *Department of Physics and Materials Research Laboratory, University of Illinois Urbana−Champaign, Urbana, Illinois 61801, United States;* orcid.org/0000-0002-3112-9734; Email: vm1@illinois.edu

Nadya Mason − *Pritzker School of Molecular Engineering, University of Chicago, Chicago, Illinois 60637, United States;* Email: nmason1@uchicago.edu

Authors

Iva Šrut Rakić − *CALT-Centre for Advanced Laser Techniques, Institute of Physics, Zagreb 10000, Croatia;* orcid.org/0000-0001-5184-8130

Matthew J. Gilbert − *Department of Electrical and Computer Engineering, University of Illinois Urbana−Champaign, Urbana, Illinois 61801, United States*

Preetha Sarkar − *Department of Physics and Materials Research Laboratory, University of Illinois Urbana−Champaign, Urbana, Illinois 61801, United States*

Anuva Aishwarya − *Department of Physics and Materials Research Laboratory, University of Illinois Urbana−Champaign, Urbana, Illinois 61801, United States*

Marco Polini − *Graphene Laboratories, Istituto Italiano di Tecnologia, Genova I-16163, Italy; Dipartimento di Fisica dell'Università di Pisa, Pisa I-56127, Italy; ICFO-Institut de Ciencies Fotoniques, The Barcelona Institute of Science and Technology, Barcelona 08860, Spain*

Complete contact information is available at: https://pubs.acs.org/10.1021/acs.nanolett.4c03542

Notes

The authors declare no competing financial interest.

■ ACKNOWLEDGMENTS

This research was supported by the NSF through the UIUC Materials Research Science and Engineering Center Grant No. DMR-2309037. I.Š.R. acknowledges financial support by the Center of Excellence for Advanced Materials and Sensing Devices (ERDF Grant No. KK.01.1.1.01.0001).

■ REFERENCES

(1) Löhneysen, H. V.; Rosch, A.; Vojta, M.; Wölfle, P. Fermi-liquid instabilities at magnetic quantum phase transitions. *Rev. Mod. Phys.* **2007**, *79*, 1015−1075.

(2) Andrei, E. Y.; Deville, G.; Glattli, D. C.; Williams, F. I. B.; Paris, E.; Etienne, B. Observation of a Magnetically Induced Wigner Solid. *Phys. Rev. Lett.* **1988**, *60*, 2765−2768.

(3) Stormer, H. L. Nobel lecture: The fractional quantum hall effect. *Rev. Mod. Phys.* **1999**, *71*, 875−889.

(4) Bolotin, K. I.; Ghahari, F.; Shulman, M. D.; Stormer, H. L.; Kim, P. Observation of the fractional quantum Hall effect in graphene. *Nature* **2009**, *462*, 196−199.

(5) Du, X.; Skachko, I.; Duerr, F.; Luican, A.; Andrei, E. Y. Fractional quantum Hall effect and insulating phase of Dirac electrons in graphene. *Nature* **2009**, *462*, 192−195.

(6) Xie, Y.; Lian, B.; Jäck, B.; Liu, X.; Chiu, C. L.; Watanabe, K.; Taniguchi, T.; Bernevig, B. A.; Yazdani, A. Spectroscopic signatures of many-body correlations in magic-angle twisted bilayer graphene. *Nature* **2019**, *572*, 101−105.

(7) Kopnin, N. B.; Heikkilä, T. T.; Volovik, G. E. High-temperature surface superconductivity in topological flat-band systems. *Phys. Rev. B* **2011**, *83*, 220503.

(8) Kauppila, V. J.; Aikebaier, F.; Heikkilä, T. T. Flat-band superconductivity in strained Dirac materials. *Phys. Rev. B* **2016**, *93*, No. 214505.

(9) Tang, E.; Fu, L. Strain-induced partially flat band, helical snake states and interface superconductivity in topological crystalline insulators. *Nat. Phys.* **2014**, *10*, 964−969.

(10) Novoselov, K. S.; Geim, A. K.; Morozov, S. V.; Jiang, D.; Katsnelson, M. I.; Grigorieva, I. V.; Dubonos, S. V.; Firsov, A. A. Two-dimensional gas of massless Dirac fermions in graphene. *Nature* **2005**, *438*, 197−200.
(11) Zhang, Y.; Tan, Y.-W.; Stormer, H. L.; Kim, P. Experimental observation of the quantum Hall effect and Berry's phase in graphene. *Nature* **2005**, *438*, 201−204.
(12) Feldman, B. E.; Krauss, B.; Smet, J. H.; Yacoby, A. Unconventional sequence of fractional quantum hall states in suspended graphene. *Science* **2012**, *337*, 1196−1199.
(13) Feldman, B. E.; Levin, A. J.; Krauss, B.; Abanin, D. A.; Halperin, B. I.; Smet, J. H.; Yacoby, A. Fractional Quantum Hall Phase Transitions and Four-Flux States in Graphene. *Phys. Rev. Lett.* **2013**, *111*, 076802.
(14) Cao, Y.; Fatemi, V.; Fang, S.; Watanabe, K.; Taniguchi, T.; Kaxiras, E.; Jarillo-Herrero, P. Unconventional superconductivity in magic-angle graphene superlattices. *Nature* **2018**, *556*, 43−50.
(15) Gao, Q.; Dong, J.; Ledwith, P.; Parker, D.; Khalaf, E. Untwisting Moiré Physics: Almost Ideal Bands and Fractional Chern Insulators in Periodically Strained Monolayer Graphene. *Phys. Rev. Lett.* **2023**, *131*, No. 096401.
(16) Mahmud, M. T.; Zhai, D.; Sandler, N. Topological Flat Bands in Strained Graphene: Substrate Engineering and Optical Control. *Nano Lett.* **2023**, *23*, 7725−7732.
(17) Manesco, A L R; Lado, J L; Ribeiro, E V S; Weber, G; Rodrigues, D, Jr. Correlations in the elastic Landau level of spontaneously buckled graphene. *2D Materials* **2021**, *8*, No. 015011.
(18) Giambastiani, D.; Colangelo, F.; Tredicucci, A.; Roddaro, S.; Pitanti, A. Electron localization in periodically strained graphene. *J. Appl. Phys.* **2022**, *131*, No. 085103.
(19) Levy, N.; Burke, S. A.; Meaker, K. L.; Panlasigui, M.; Zettl, A.; Guinea, F.; Neto, A. H. C.; Crommie, M. F. Strain-Induced Pseudo-Magnetic Fields Greater Than 300 T in Graphene Nanobubbles. *Science* **2010**, *329*, 544−547.
(20) Milovanović, S. P.; Andelković, M.; Covaci, L.; Peeters, F. M. Band flattening in buckled monolayer graphene. *Phys. Rev. B* **2020**, *102*, No. 245427.
(21) Phong, V. T.; Mele, E. Boundary Modes from Periodic Magnetic and Pseudomagnetic Fields in Graphene. *Phys. Rev. Lett.* **2022**, *128*, No. 176406.
(22) Ghaemi, P.; Cayssol, J.; Sheng, D. N.; Vishwanath, A. Fractional Topological Phases and Broken Time-Reversal Symmetry in Strained Graphene. *Phys. Rev. Lett.* **2012**, *108*, No. 266801.
(23) Yeh, N. C.; Teague, M. L.; Yeom, S.; Standley, B. L.; Wu, R. T.; Boyd, D. A.; Bockrath, M. W. Strain-induced pseudo-magnetic fields and charging effects on CVD-grown graphene. *Surf. Sci.* **2011**, *605*, 1649−1656.
(24) Mao, J.; Milovanović, S. P.; Andelković, M.; Lai, X.; Cao, Y.; Watanabe, K.; Taniguchi, T.; Covaci, L.; Peeters, F. M.; Geim, A. K.; Jiang, Y.; Andrei, E. Y. Evidence of flat bands and correlated states in buckled graphene superlattices. *Nature* **2020**, *584*, 215−220.
(25) Faria, D.; León, C.; Lima, L. R.; Latgé, A.; Sandler, N. Valley polarization braiding in strained graphene. *Phys. Rev. B* **2020**, *101*, No. 081410.
(26) Li, S. Y.; Su, Y.; Ren, Y. N.; He, L. Valley Polarization and Inversion in Strained Graphene via Pseudo-Landau Levels, Valley Splitting of Real Landau Levels, and Confined States. *Phys. Rev. Lett.* **2020**, *124*, No. 106802.
(27) Forsythe, C.; Zhou, X.; Watanabe, K.; Taniguchi, T.; Pasupathy, A.; Moon, P.; Koshino, M.; Kim, P.; Dean, C. R. Band structure engineering of 2D materials using patterned dielectric superlattices. *Nat. Nanotechnol.* **2018**, *13*, 566−571.
(28) Li, Y.; Dietrich, S.; Forsythe, C.; Taniguchi, T.; Watanabe, K.; Moon, P.; Dean, C. R. Anisotropic band flattening in graphene with one-dimensional superlattices. *Nat. Nanotechnol.* **2021**, *16*, 525−530.
(29) Zhang, Y.; Kim, Y.; Gilbert, M. J.; Mason, N. Magnetotransport in a strain superlattice of graphene. *Appl. Phys. Lett.* **2019**, *115*, No. 143508.
(30) Zhang, Y.; Heiranian, M.; Janicek, B.; Budrikis, Z.; Zapperi, S.; Huang, P. Y.; Johnson, H. T.; Aluru, N. R.; Lyding, J. W.; Mason, N. Strain Modulation of Graphene by Nanoscale Substrate Curvatures: A Molecular View. *Nano Lett.* **2018**, *18*, 2098−2104.
(31) Zhang, Y.; Kim, Y.; Gilbert, M. J.; Mason, N. Electronic transport in a two-dimensional superlattice engineered via self-assembled nanostructures. *npj 2D Materials and Applications* **2018**, *2*, 31.
(32) Zhang, Y.; Brar, V. W.; Girit, C.; Zettl, A.; Crommie, M. F. Origin of spatial charge inhomogeneity in graphene. *Nat. Phys.* **2009**, *5*, 722−726.
(33) Zhang, Y.; Brar, V. W.; Wang, F.; Girit, C.; Yayon, Y.; Panlasigui, M.; Zettl, A.; Crommie, M. F. Giant phonon-induced conductance in scanning tunnelling spectroscopy of gate-tunable graphene. *Nat. Phys.* **2008**, *4*, 627−630.
(34) Georgi, A.; Nemes-Incze, P.; Carrillo-Bastos, R.; Faria, D.; Viola Kusminskiy, S.; Zhai, D.; Schneider, M.; Subramaniam, D.; Mashoff, T.; Freitag, N. M.; Liebmann, M.; Pratzer, M.; Wirtz, L.; Woods, C. R.; Gorbachev, R. V.; Cao, Y.; Novoselov, K. S.; Sandler, N.; Morgenstern, M. Tuning the Pseudospin Polarization of Graphene by a Pseudomagnetic Field. *Nano Lett.* **2017**, *17*, 2240−2245.
(35) Zhai, D.; Sandler, N. Electron dynamics in strained graphene. *Modern Physics Letters B* **2019**, *33*, No. 1930001.
(36) Schneider, M.; Faria, D.; Viola Kusminskiy, S.; Sandler, N. Local sublattice symmetry breaking for graphene with a centrosymmetric deformation. *Phys. Rev. B* **2015**, *91*, No. 161407.
(37) Banerjee, R.; Nguyen, V. H.; Granzier-Nakajima, T.; Pabbi, L.; Lherbier, A.; Binion, A. R.; Charlier, J. C.; Terrones, M.; Hudson, E. W. Strain Modulated Superlattices in Graphene. *Nano Lett.* **2020**, *20*, 3113−3121.
(38) Teague, M. L.; Lai, A. P.; Velasco, J.; Hughes, C. R.; Beyer, A. D.; Bockrath, M. W.; Lau, C. N.; Yeh, N.-C. Evidence for Strain-Induced Local Conductance Modulations in Single-Layer Graphene on SiO 2. *Nano Lett.* **2009**, *9*, 2542−2546.
(39) Manesco, A. L. R.; Lado, J. L. Correlation-induced valley topology in buckled graphene superlattices. *2D Materials* **2021**, *8*, No. 035057.
(40) Abanin, D. A.; Pesin, D. A. Interaction-Induced Topological Insulator States in Strained Graphene. *Phys. Rev. Lett.* **2012**, *109*, No. 066802.

https://doi.org/10.1021/acs.nanolett.4c03542
Nano Lett. 2025, 25, 41−47